

# Structural, optical and photo luminescence studies on N-acetylglycine single crystal

V. J. THANIGAIARASU<sup>a</sup>, N. KANAGATHARA<sup>b,\*</sup>, K. SENTHILKUMAR<sup>c</sup>, G. ANBALAGAN<sup>d</sup>,  
M. K. MARCHEWKA<sup>e</sup>

<sup>a</sup>Department of Physics, Jaya College of Arts and Science, Thiruninravur, Chennai 602 024, India

<sup>b</sup>Department of Physics, Saveetha School of Engineering, Saveetha Institute of Medical and Technical Sciences, Thandalam, Chennai 602 105, India

<sup>c</sup>Department of Physics, Rajalakshmi Engineering College, Thandalam, Chennai 602 105, India

<sup>d</sup>Department of Nuclear Physics, University of Madras, Guindy Campus, Chennai 600 025, India

<sup>e</sup>Institute of Low Temperature and Structure Research, Polish Academy of Sciences, 50-950, Wrocław, 2, P.O. Box 937, Poland

The crystals of N-acetylglycine (NAG) had been obtained through the gradual evaporation of an aqueous solution at room temperature. Single crystal X-ray diffraction analysis let out that the crystal associated to monoclinic system with centro symmetric space group  $P2_1/c$ . The lattice parameters are calculated to be  $a=4.8410(10)$  Å,  $b=11.512(2)$  Å,  $c=9.810(2)$  Å,  $\alpha=90^\circ$ ,  $\beta=97.02(3)^\circ$ ,  $\gamma=90^\circ$  and  $V=542.61$  (Å)<sup>3</sup>. The primitive unit cell has 4 molecules. Vibrational spectroscopic analysis is reported on the basis of FT-IR and FT-Raman spectra recorded at room temperature. The crystal gives notable vibrational effect due to the presence of extensive hydrogen bond network. The UV-Vis studies have been carried out and the cutoff wavelength  $\lambda$  is observed to be 379 nm. The energy gap is calculated as 2.757 eV. The luminescence property has been examined by Photo luminescence spectrum. Thus in the existing study, structure-property correlation of n-acetylglycine molecule is investigated for future nonlinear optical purposes through experimental approach.

(Received October 28, 2019; accepted August 18, 2020)

**Keywords:** XRD, UV-Vis, Vibrational, Band gap, Photo luminescence

## 1. Introduction

Nonlinear Optical materials play a versatile position in the area of Photonic and Opto electronic applied sciences due to their ample NLO response. Amino acid crystals are bio-organic materials with promising applications in UV and IR detectors and non-linear optics due to their zwitterion nature i.e the presence of amino group  $\text{NH}_3^+$  and the carboxylic group  $\text{COO}^-$ . N-acetylglycine (NAG) is the N-acetylated derivate of the proteinogenic chiral amino acid. It can be biosynthesized in the human body by enzymes starting from serine and tetrahydrofolate [1] and known to be a minor constituent of numerous foods. Also it is the chemical building block for compounds such as glycine, aspartame and other amino acids. It is extensively used in peptidomimetics and drug research. Its methyl ester can replace menthol in oral care products and its salts are able to elicit umami taste in food products. Theoretically the vibrational spectral and molecular structure of N-acetylglycine oligomers and polyglycine were studied by Saba Bee et al. [2]. The conformational properties of N-acetylglycine are studied by Bram Boecks and Guido Maes [3]. DFT-B3LYP/6-311++G(d,p) basis set is applied to get the vibrational spectrum of N-acetyl L alanine by Bruyneel et al [4]. The dielectric and ferroelectric properties of N-acetylglycine phosphite was studied by

Vizhi et al [5] and further it was deeply analyzed by Baran et al [6]. Harsh Kumar et al studied the physico-chemical properties of N-acetylglycine at different temperatures [7]. Rafael Notaria et al studied the computational study of N-acetyl L-cysteine [8]. Molecular structure, vibrational spectra and DFT computational studies of melaminium N-acetylglycinate dihydrate was investigated by Tanak et al [9]. Crystal structure of N-acetyl glycine was already reported [10]. Jerry Donohue studied the refinement structure of N-acetyl glycine [11]. The infrared spectrum of N-acetylglycine was reported by many researchers [3, 12]. Thus lot of works were made to explain the N-acetylglycine molecule in the solid state in various theoretical and experimental aspects. In the present communication, spectral, absorption spectra and photoluminescence of pure N-acetyl glycine crystals are studied and discussed in detail.

## 2. Experimental

Crystals of N-acetylglycine [ $\text{C}_4\text{H}_7\text{NO}_3$ ] were obtained by crystallization of AR grade samples of N-acetylglycine aqueous solution by the slow evaporation process at room temperature and the pH value is measured as 1. During a

few days, tiny colourless crystals were produced. The picture of the crystals is shown in Fig. 1.

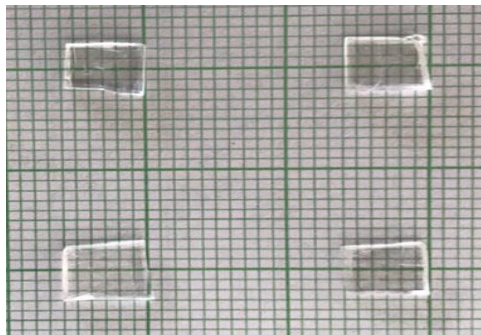


Fig. 1. Photograph of as grown crystals NAG (color online)

### 3. Results and discussion

#### 3.1. Single crystal X-ray Diffraction analysis

The grown crystals of NAG was exposed to single crystal XRD analysis using KUMA KM-4 single crystal X-ray diffractometer geared up with a two-dimensional area CCD detector with  $M_oK_{\alpha}$  ( $\lambda=0.71073 \text{ \AA}$ ) radiation. The single crystal XRD report of NAG indicates that it crystallizes in the monoclinic system with centro symmetric space group  $P2_1/c$  with lattice  $a=4.8410(10) \text{ \AA}$ ,  $b=11.512(2) \text{ \AA}$ ,  $c=9.810(2) \text{ \AA}$ ,  $\alpha=90^\circ$ ,  $\beta=97.02(3)^\circ$ ,  $\gamma=90^\circ$  and  $V=542.61 \text{ (\AA)}^3$ . Table 1 furnishes the structure refinement parameters of NAG crystal. Selected bond distances and bond angles are given in Table 2. Fig.2 and 3 represents the ORTEP and packing diagram of grown NAG crystal.

Table 1. Crystal data and structure refinement for *N*-acetyl glycine (NAG)

Empirical formula	C <sub>4</sub> H <sub>7</sub> N O <sub>3</sub>
Formula weight (g mol <sup>-1</sup> )	117.11
Temperature (K)	293(2)
Wavelength (Å)	0.71073 Å
Crystal system	monoclinic
Space group	$P2_1/c$
a	4.8410(10) Å
b	11.512(2) Å
c	9.810(2) Å
$\alpha$	90°
$\beta$	97.02(2)°
$\gamma$	90°
V	542.61(19) (Å) <sup>3</sup>
Z	4
$D_{\text{calc}}$ (Mg m <sup>-3</sup> )	1.434
Absorption coefficient (mm <sup>-1</sup> )	0.123

F(000)	248
Crystal size (mm)	0.21 x 0.13x 0.12
Theta range for data collection (°)	2.74-29.54
Index ranges	$h=-5 \rightarrow 6$ ; $k=-15 \rightarrow 15$ ; $l=-13 \rightarrow 11$
Completeness to $\theta$	100%
Refinement method	Full-matrix least squares on F <sup>2</sup>
Data/restraints/parameters	1413/0/80
Goodness of fit on F <sup>2</sup>	1.076
Largest differences peak and hole (e.Å <sup>-3</sup> )	0.866 and -1.030

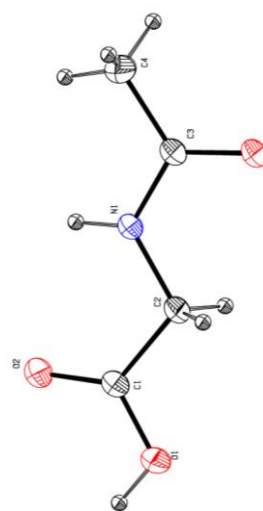


Fig. 2. ORTEP diagram of NAG (color online)

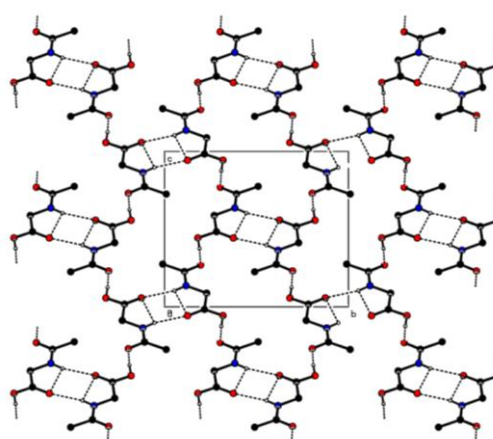


Fig. 3. Packing diagram of NAG (color online)

Table 2. Selected bond distances ( $\text{\AA}$ ) and bond angles ( $^\circ$ ).

Atom	Bond distance ( $\text{\AA}$ )	Atom	Bond angle ( $^\circ$ )	Atom	Bond angle ( $^\circ$ )
O1-C1	1.304	C1-O1- H1	110.0	C3-C4-H42	109.5
O1-H1	0.900	O2-C1- O1	125.1	H41-C4-H42	109.5
O2-C1	1.197	O2- C1- C2	123.4	C3-C4-H43	109.5
C1- C2	1.503	O1-C1- C2	111.5	H41-C4-H43	109.5
C2-N1	1.438	N1- C2- C1	110.8	H42-C4-H43	109.5
C2-H21	0.970	N1-C2- H21	109.5	O3-C3-C4	122.3
C2-H22	0.970	C1-C2-H21	109.5	N1-C3-C4	117.6
N1-C3	1.329	N1-C2- H22	109.5	C3-C4-H41	109.5
N1- H2	0.850	C1-C2-H22	109.5	C3-N1-H2	117.1
C3-O3	1.232	H21-C2- H22	108.1	C2-N1-H2	122.1
C3-C4	1.483	C3-N1-C2	120.6	O3-C3-N1	120.1
C4-H41	0.960				
C4-H42	0.960				
C4-H43	0.960				

### 3.2. X-ray powder diffraction analysis

The grown crystals have been described by X-ray powder diffraction procedure using Panalytical Empyrean X-ray powder diffractometer with  $\text{CuK}\alpha$  radiation of  $\lambda=1.5406 \text{ \AA}$ . The  $2\theta$  range was analyzed from  $10^\circ$  to  $70^\circ$  by employing the reflection mode for scanning.

The scintillation counter was used as a detector.

Fig. 4 shows the X-ray Powder diffraction pattern for the grown crystal. From the X-ray powder diffraction data, the lattice parameters and the cell volume have been calculated and are found to be  $a = 4.9232 \pm 0.0204 \text{ \AA}$ ,  $b = 11.4162 \pm 0.0395 \text{ \AA}$ ,  $c = 9.8134 \pm 0.0229 \text{ \AA}$ ,  $\alpha = \gamma = 90^\circ$ ,  $\beta = 97.70^\circ$  and volume  $V = 546.581 (\text{ \AA})^3$ . These reveal a close agreement with the values obtained from the single crystal x-ray diffraction. The prominent peaks are identified and indexed.

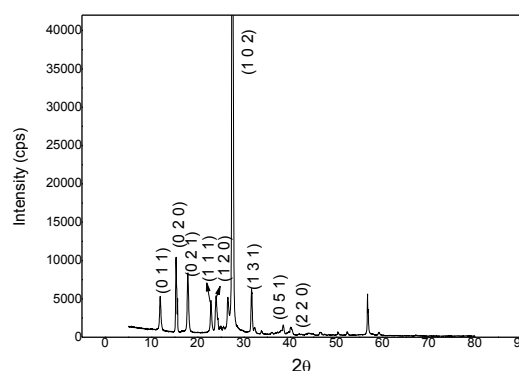


Fig. 4. Experimental X-ray powder diffraction spectrum

### 3.3. Simulated X-ray powder diffraction analysis

Theoretically the crystalline nature of the grown crystal can be identified by powder X-ray diffraction analysis with the help of with the help of Mercury 3.8 software. Fig. 5 depicts the simulated powder X-ray diffraction spectrum of the grown crystal. Debye-Scherrer's formula is used to calculate the crystallite size (D) of NAG by using equation

$$D = K\lambda / (\beta_{1/2} \cos\theta)$$

where  $K=0.89$ ,  $\lambda=1.5405 \text{ \AA}$  and  $\beta_{1/2}$  is the peak width of the reflection at half intensity. The maximum intensity peak is observed at  $2\theta=27.70^\circ$ . The average value of the crystallite size of NAG is found to be  $14.12 \mu\text{m}$ .

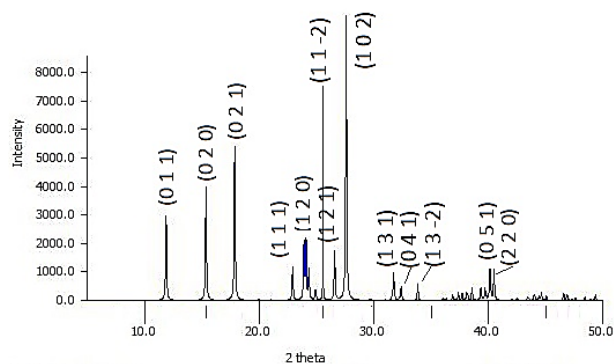


Fig. 5. Simulated X-ray powder diffraction spectrum (color online)

### 3.4. Vibrational spectral analysis

Vibrational spectroscopy is an effective tool to elucidate the structural characterization of the compounds. The vibrational measurements were made at room temperature. Bruker IFS-88 spectrometer is used to record infrared spectra in the region  $4000\text{--}80 \text{ cm}^{-1}$  while FRA-106 attachment to the Bruker IFS-88 spectrometer equipped with Ge detector cooled to liquid nitrogen temperature is used to record powder Fourier Transform Raman (FT Raman) spectra with an Resolution was set up to  $2 \text{ cm}^{-1}$ .  $\text{Nd}^{3+}$ :YAG air-cooled diode pumped laser of power of  $200\text{mW}$  was used as an exciting source. The incident laser excitation is  $1064 \text{ nm}$ . The scattered light was collected at the angle of  $180^\circ$  in the region  $3600\text{--}80 \text{ cm}^{-1}$ , resolution  $2 \text{ cm}^{-1}$ , 256 scans. Figs. 6 and 7 gives the FT-IR and FT Raman spectrum of the grown NAG crystal.

The grown crystal has various functional groups viz. C-C, C-N, N-H, C-H, O-H. The interpretation of the both IR and Raman spectra of NAG is presented and discussed below. The strong infrared peak and weak peak at  $3355$  and  $3260 \text{ cm}^{-1}$  is attributed to NH symmetric stretching vibration [13]. The medium peaks at  $2925$  and  $2852 \text{ cm}^{-1}$  are ascribed to CH asymmetric stretching vibration. The corresponding Raman counterpart occurs at  $2937 \text{ cm}^{-1}$  with medium intensity [2]. The carboxylic group appears its presence at  $1722 \text{ cm}^{-1}$  with medium intensity in infrared spectrum. Its Raman counterpart appears at  $1710 \text{ cm}^{-1}$  with weak intensity. The acetyl group of  $\text{COO}^-$  asymmetric

stretching vibration occurs at  $1583 \text{ cm}^{-1}$  with strong intensity [13]. N-H in-plane bending vibration occurs at  $1547$ ,  $1350 \text{ cm}^{-1}$  with strong IR intensity and  $1554 \text{ cm}^{-1}$  with weak Raman intensity [2]. Also the peak at  $693/682 \text{ cm}^{-1}$  in IR/Raman is nominated to  $\text{NH}_2$  bending vibration. The infrared peaks at  $1437$ ,  $1379$ ,  $1226$  and  $1146 \text{ cm}^{-1}$  as well as Raman peaks at  $1441$ ,  $1377$ ,  $1228$  and  $1136 \text{ cm}^{-1}$  are referred to  $\text{CH}_3$  and  $\text{CH}_2$  bending vibration [2,13]. The bending vibration of  $\text{COO}^-$  occurs at  $600, 548$  and  $410 \text{ cm}^{-1}$  in infrared spectrum with weak intensity. Their Raman counterpart occurs at  $590$ ,  $555, 505$  and  $397 \text{ cm}^{-1}$  with intensity [13].

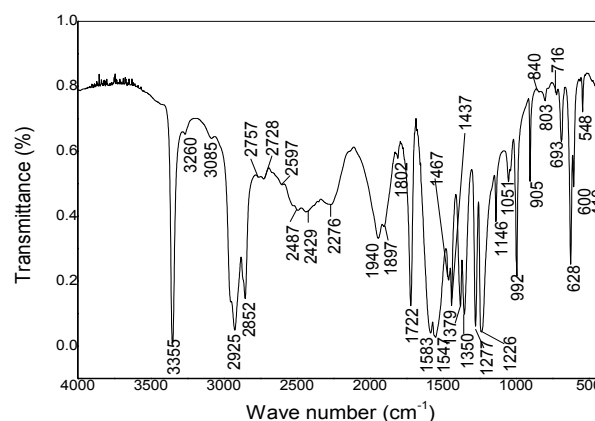


Fig. 6. FT-IR spectrum of NAG

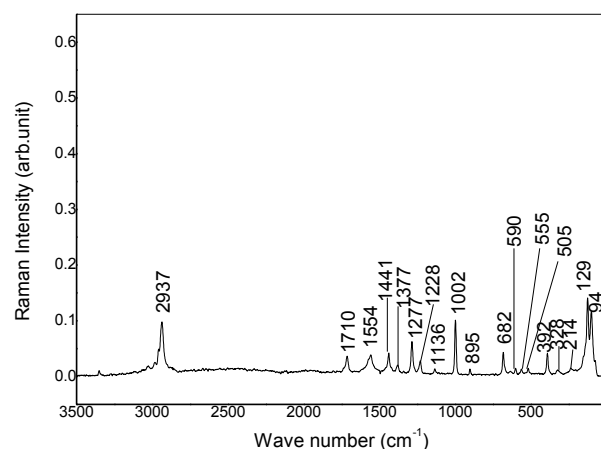


Fig. 7. FT Raman spectrum of NAG

Table 3. Detailed assignments of experimental wavenumbers of NAG

FT-IR (cm <sup>-1</sup> )	FT-Raman (cm <sup>-1</sup> )	Band Assignment Description
3355 vs		N-H asymmetric stretching
3260 w		N-H symmetric stretching
3085w		C-H asymmetric stretching
2925 m	2937 m	asymmetric C-H stretching
2852 m		asymmetric C-H stretching
1722 m	1710 w	carboxyl C=O
1583 s		acetyl COO <sup>-</sup> asymmetric stretching
1547 s	1554 w	N-H in plane bending
1467 s		CH <sub>3</sub> asymmetric bending
1437 m	1441 w	CH <sub>3</sub> and CH <sub>2</sub> bands
1379 m	1377 w	CH <sub>3</sub> symmetric bending, O-C-O bending
1350 m		NH <sub>2</sub> bend, CH <sub>2</sub> wagging, twisting
1277 m		NH <sub>2</sub> wagging
1226 w	1228 w	CH <sub>3</sub> bands
1146 m	1136 m	CH <sub>3</sub> bands
1051 m		C-N-C stretching
992 m	1002 s	C-N-C stretching
905 m	895 vw	C-N-C stretching
840 w		C-C asymmetric stretching
716 w		C-N-C bending
693 m	682 w	NH <sub>2</sub> bending
628 ms		C-N, C=O stretching
600 w	590 w	COOH bending, NCCO bend
548 w	555 w	COO <sup>-</sup> deformation
	505 w	C=O bending, C-N bending
410 w	397 w	COO <sup>-</sup> rocking
	328 w	CCN bending
	214 w	CNC bending
	129 s	CCN/CNC bending
	94 s	Lattice vibration

**Abbreviations:** vs-very strong; s-strong; ms-medium strong, m-medium, w-weak; vw-very weak

### 3.5. Optical absorption studies

Perkin Elmer Lambda 35 Spectrophotometer records the UV-Visible spectrum in the region 200-800 nm. The transition of electrons in  $\sigma$  and  $\pi$  orbital from the ground state to higher energy states due to the absorption of UV and visible light gives information about the structure of the molecule. Wide range of transmission in transmission spectral analysis is important for any material to possess non linear optical activity. The two bands at 232 and 379 nm in the electronic absorption spectrum indicates the  $\pi$ - $\pi^*$  transitions in C=N due to intra molecular charge

transfer in the molecule [14]. Also from the spectrum (Fig.8), it is clear that the title crystal has UV cutoff wavelength at 379 nm which is ample for SHG laser radiation or other appliance in the blue region [15].

The absorption coefficient is calculated using

$$\alpha = \frac{2.3026 \log\left(\frac{I_0}{I}\right)}{t}$$

The optical band gap ( $E_g$ ) was calculated from the transmission spectra and the optical absorption coefficient ( $\alpha$ ) near the absorption edge is given by

$$h\nu\alpha = A(h\nu - E_g)^{1/2}$$

where A - constant,  $E_g$  - the optical band gap, h - the Plank's constant and  $\nu$  - the frequency of the incident photons. Tauc's relation gives the direct band gap values by plotting a graph between  $h\nu$  and  $(\alpha h\nu)^2$ , where  $\alpha$  is the absorption coefficient and  $h\nu$  is the energy of the incident photon  $E=h\nu$  and it is shown in Fig.8 (inset). The energy gap  $E_g$  is determined by extrapolating the straight line portion of the curve to  $(\alpha h\nu)^2 = 0$ . From the plot, the band gap of the grown crystal is found to be 2.757 eV. Thus the

minimum absorbance near IR region and visible region plays a major role in NLO applications. Optical parameters has major role while fabricating the opto electronic devices. The wavelength vs refractive index relation for NAG in depicted in Fig.9. The refractive index for NAG is established to be 1.38 throughout the visible region suggesting the material suitable for fabrication of NLO and solar thermal devices applications [16].

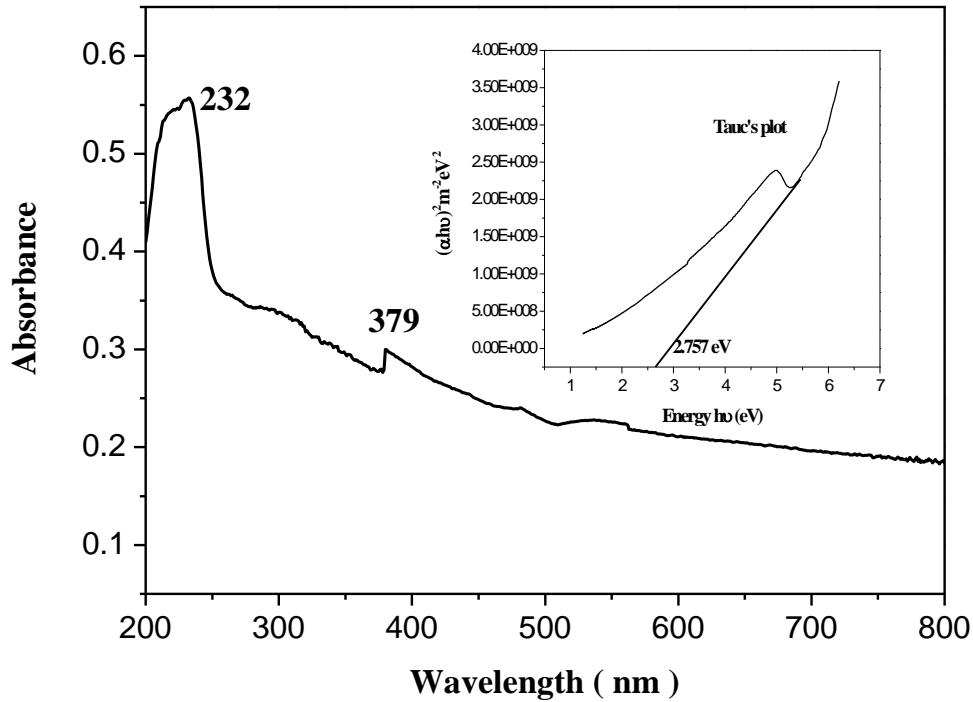


Fig. 8. UV-Vis spectrum and Tauc's plot (inset) of NAG

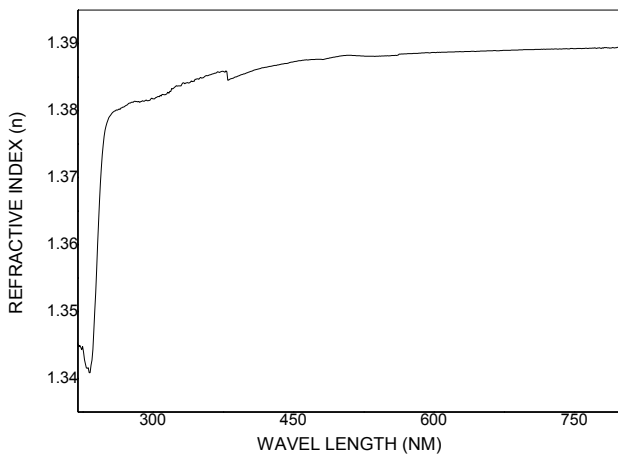


Fig. 9. Refractive index vs wavelength of NAG crystal

### 3.6. Photo luminescence studies

The photoluminescence (PL) spectral analysis gives the complete information about the physical properties at the molecular level as well as the presence of deep and shallow level defects of materials. The photoluminescence (PL) measurement was performed in the range 300-800 nm on NAG crystal using a Perkin Elmer Spectrofluorometer with 450W high pressure xenon lamp as an excitation source. The sample was excited at 232, 280 and 310 nm based on UV absorption and the recorded PL emission spectrum is shown in Fig. 10. There are three emission peaks appeared at 396, 562 and 622 nm and observed that the emission peak intensity decreases after reaches the maximum intensity. The PL intensity is highly reliant on the crystallinity and structural perfection of the crystal. Hence the photoluminescence studies confirm the suitability of the grown material for near violet to orange fluorescence emission depends upon the excitation and may be found to be more competent for OLED applications and optical data storage applications [17, 18].

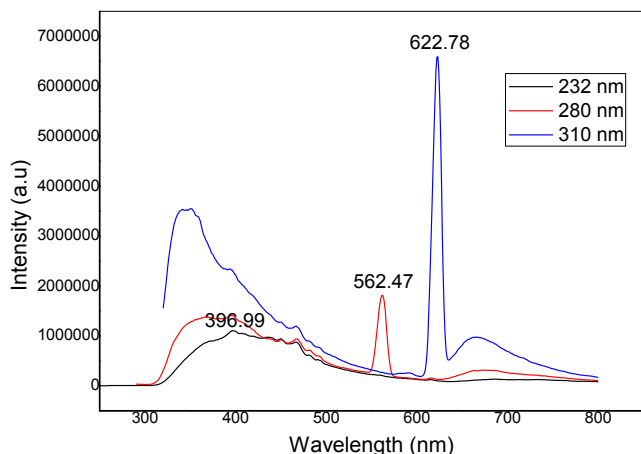


Fig. 10. Photo luminescence spectrum of NAG (color online)

#### 4. Conclusion

Single crystals of N-acetylglycine (NAG) were developed by the slow evaporation of an aqueous solution at room temperature. Single crystal X-ray diffraction assay affirm that the crystal crystallizes in monoclinic system with centro symmetric space group  $P2_1/c$ .

The lattice parameters are  $a=4.8410(10)$  Å,  $b=11.512(2)$  Å,  $c=9.810(2)$  Å,  $\alpha=90^\circ$ ,  $\beta=97.02(3)^\circ$ ,  $\gamma=90^\circ$  and  $V=542.61$  (Å)<sup>3</sup>. There are 4 molecules per primitive unit cell. The various functional groups present in the crystal are identified by FT-IR and FT Raman spectral analysis. The UV-Vis studies have been carried out and the cutoff wavelength  $\lambda$  is found to be 379 nm. The optical band gap is calculated as 2.757 eV. The refractive index for NAG is found to be 1.38 throughout the visible region which suggests that this material is suitable for fabrication of solar thermal devices and NLO applications. The Photo luminescence spectrum studies affirm the appropriateness of the grown material for applications in OLED s and optical data storage. Thus in the present investigation, structure-property relationship of novel n-acetylglycine molecule is studied for future nonlinear optical applications through experimental approach.

#### References

- [1] D. L. Nelson, M. M. Cox, Principles of Biochemistry, 4th ed., Freeman, Boston, 2005.
- [2] Saba Bee, Neetu Choudhary, Archana Gupta, Poonam Tandon, Biopolymers **101**, 795 (2013).
- [3] Bram Boeckx, Guido Maes, J. Phys. Chem. A **116**, 1956 (2012).
- [4] C. Bruyneel, Asit K. Chandra, T. Uchimar, Th. Zeegers-Huyskens, Spectrochimica Acta A **56**, 591 (2000).
- [5] R. E. Vizhi, R. A. Kumar, D. R. Babu, K. Sathiyarayanan, G. Bhagavannarayana, Ferroelectrics **413**, 291 (2011).
- [6] J. Baran, A. M. Petrosyan, Comments on the Paper by R. Ezhil Vizhi et al., Ferroelectrics **432**, 117 (2015).
- [7] Harsh Kumar, Meenu Singla, Heena Mittal, J. Chem. Thermodynamics **94**, 204 (2016).
- [8] Rafael Notario, María Victoria Roux, Ana Filip, L. O. M. Santos Maria, D. M. C. Ribeiro da Silva, J. Chem. Thermodynamics **73**, 57 (2014).
- [9] H. Tanak, K. Pawlus, M. K. Marchewka, J. Mol. Struc. **1121**, 142 (2016).
- [10] G. B. Carpenter, J. Donohue, The Crystal Structure of N-acetyl glycine, J. Am. Chem. Soc. **72**, 2315 (1950).
- [11] Jerry Donohue, Acta Cryst **15**, 941 (1962).
- [12] H. Etori, K. Taga, H. Okabayashi, K. Ohshima, J. Chem. Soc. Faraday Trans. **93**, 313 (1997).
- [13] Roger Newman and Richard M. Badger, J. Chem. Phys. **19**, 1147 (1951).
- [14] Hasan Tanak, Levent Semiz, Figen Koçak, Ayşen Alaman Açar, Namık Özdemir, Optik - International Journal for Light and Electron Optics **195**, 163144 (2019).
- [15] R. Usha, N. Hema, V. Revathi Ambika, D. Shalini, D. Jayalakshmi, Asian J Chem, **30**(2), 343 (2018).
- [16] Ollaa M. Mailouda, Adly H. Elsayedb, A. H. Abo-Elazmb, H. A. Fetouh, Results Phys. **10**, 512 (2018).
- [17] K. J. Arun, S. Jayalekshmi, J. Miner. Mater. Charact. Eng. **8**(8), 635 (2009).
- [18] R. Usha, N. Hema, V. Revathi Ambika, D. Shalini, D. Jayalakshmi, Mater. Res. Innov, 1 (2017).

\* Corresponding author: kanagathaara@gmail.com